Chinese Chemical Letters 31 (2020) 2921–2924

Contents lists available at ScienceDirect

Chinese Chemical Letters

journal homepage: www.elsevier.com/locate/cclet

Communication

Circularly polarized luminescence induced by excimer based on pyrene-modified binaphthol

Chaoyang Wang, Tao Jiang, Xiang Ma*

Key Laboratory for Advanced Materials and Feringa Nobel Prize Scientist Joint Research Center, Institute of Fine Chemicals, School of Chemistry and Molecular Engineering, East China University of Science and Technology, Shanghai 200237, China

ARTICLE INFO

Article history:
Received 4 February 2020
Received in revised form 6 March 2020
Accepted 6 March 2020
Available online 7 March 2020

Keywords:
Chirality
Excimer
Circularly polarized luminescence
Aggregated induced emission
Binaphthol

ABSTRACT

A new chiral bromobinaphthol-pyrene compound was developed to achieve a green circularly polarized luminescence (CPL) from its excimer with a dissymmetry factor ($|g_{lum}|$) value of 4.3×10^{-3} and a high quantum yield $\Phi_{F, solid}$ up to 55.9%, while no CPL signals could be observed for the blue luminescence from unimolecule. Meanwhile, reversal CPL signals can be observed from both concentrated solution and solid

Organic luminescent materials have been attracting great attention due to its peculiar optical properties and potentials in various practical applications [1–7]. Particularly, circularly polarized luminescence (CPL) was derived from the chiral luminophor or in chiral environments, presenting great potentials in asymmetric synthesis [8,9], biological probes [10,11], optical device [12,13], 3D display [14] and so on. The degree of dissymmetry of CPL is usually evaluated in terms of the luminescence factor (dissymmetry g_{lum}) which is calculated by the equation $g_{lum} = 2(I_L - I_R)/(I_L + I_R)$ demonstrated the relative intensity difference of left and right circularly polarized emission. Therefore, one of the challenges of luminescent materials is to obtain a high luminescence dissymmetry factor g_{lum} and high quantum yield (Φ_F).

To date, numerous methods such as assemblies [15–20], chiral metal complexes [21], chiral aggregation-induced emission (AIE)-active chromophores [22], liquid crystals [23], host-guest interaction [24,25] and CT complexes [26] have been developed. Those methods can not only realize the CPL, but also amplify chiral signal. Despite those impressive reports, there are still some problems. Intensive CPL signals can be observed for assemblies due to chirality amplify accompanying the low luminescence efficiency. Chiral metal complexes have been extensive studied since CPL was observed for lanthanide complexes. The majority of metal complexation exhibited the high dissymmetry factor g_{lum} value but small Φ_F due to the involved metal-centred electronic transition limiting their potentials. Chiral AIE-active chromophores combined the aggregation-induced emission with CPL have been studied due to alternative emission and potentials in circularly polarized organic light emitting diodes. Liquid crystal and CT complexes require sophisticated design solutions and strict experiment condition hindering their application.

Binaphthol and its derivatives have attracted a lot of attention due to the intrinsic chiral texture derived from the restricted rotation of two naphthalene rings. Moreover, the flexibility of binaphthol leads to the variation in properties and application such as regulating CPL signals [27,28], CPL switch [29], host – guest complex [30,31] and excimer [32–34]. Herein, we developed a chiral material based on binaphthol and pyrene unit with both high dissymmetry factors g_{lum} and high Φ_F. Binaphthol was chosen as chiral core due to its inherent chirality and easy-modification. The pyrene unit was chosen to obtain high fluorescence quantum yield. Our study demonstrated that the material possessed peculiar optical properties with both relatively high dissymmetry factor g_{lum} and quantum yield Φ_F and reversal CPL signals in different states. The compound was demonstrated in Scheme 1. Compound *R/S*-**2** was synthesised *via* the esterification of brominated binaphthol and pyrene formic acid. The detailed procedures and characterization referred to Supporting information. The enantiomer pairs were readily prepared in quantity. The materials were yellow solid and had good solubility in regular solvents. Meanwhile, it had disparate emission phenomena in different concentrations. In a diluted solution, the PL intensity was conspicuous while CPL was almost not observed. In the

* Corresponding author.
E-mail address: maxiang@ecust.edu.cn (X. Ma).

https://doi.org/10.1016/j.cclet.2020.03.021
1001-8417/

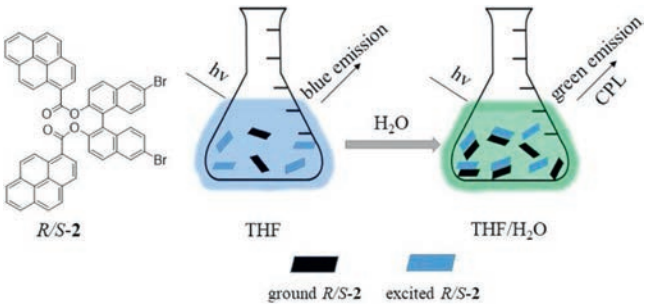

Scheme 1. Structure of *R*/*S*-**2** and emission in THF and THF/H_2O.

concentrated solution, the PL intensity was weak but CPL signal was strong. More importantly, the addition of H_2O resulted in a green emission with a maximum Φ_F 27.6% and strong CPL signal. The dissymmetry factor $|g_{lum}|$ value of the chiral material was up to 6×10^{-3} in this mixture solvent.

To evaluate the optical properties of solid *R*/*S*-**2**, the fluorescence, absorption and CPL spectra were detected and shown in Fig. 1. The fluorescence spectrum showed the only emission peak at 510 nm. The solid absorption spectrum had a broad band around 250−500 nm. The solid CPL spectra was characterized in smooth film and exhibited distinct CPL signal with a high dissymmetry factor $|g_{lum}|$ value of 4.3×10^{-3} and a high quantum yield $\Phi_{F,\ solid}$ 55.9%. XRD (Fig. S8 in Supporting information) was conducted to explore the morphology of the *R*/*S*-**2** solid and the result showed that the *R*/*S*-**2** solids were amorphous.

The enantiomer *S*-**2** was selected as a sample and its photophysical spectra were thoroughly investigated. The corresponding spectra of *R*-**2** could be referred to Supporting information. The absorption spectra of *S*-**2** had been detected in THF solvent (Fig. 2a). The UV–vis absorption of *S*-**2** had three distinct peaks at 283, 352 and 383 nm respectively, accompanying with a weak shoulder peak at 272 nm. The peaks at 352 and 383 nm were assigned to the pyrene moieties. When the concentration increased to 1×10^{-4} mol/L, the peaks at 352 and 383 nm had a bathochromic shift to 356 and 387 nm, respectively. Such an bathochromic effect was an indication of aggregate formation, which in turns had a favourable geometry to exhibit excimer emission [35]. Compared with solid state, its THF solution was colourless and had a blue fluorescence emission. In Fig. 2b, the fluorescence spectra of *S*-**2** had two distinct peaks at 387 and 408 nm along with a weak shoulder peak at 428 nm. Furthermore, the increase in concentration resulted in a sharp decrease in the intensity of PL. The chirality properties of *R*/*S*-**2** were examined by circular dichroism (CD) spectra (Fig. 2c). The CD spectra exhibited mirror-image bands indicating that *R*/*S*-**2** were a pair of enantiomers. The strong Cotton effects at 240 and 280 nm in the short wavelength region were assigned to the characteristic absorption of chiral binaphthyl moieties [36]. The cotton effects at 360 nm in concentrated solution were attributed to the pyrene units [37]. CPL spectra (Fig. 2d) showed there was no obvious signal in the range of 400−700 nm at 1×10^{-5} mol/L. After increasing the concentration, a characteristic band around 470−650 nm could be observed, which was due to the formation of excimer [38]. In the diluted solution (Fig. 2b), the emission at 387, 408 and 428 nm represented the emission from single molecules and no obvious CPL signal could be observed. While in concentrated solution, the emission derived from excimer appeared accompanying with a strong CPL signal. The dissymmetry factor ($|g_{lum}|$) value was up to 6×10^{-2} and the quantum yield was 1.7%. Notably, reversal CPL signal can be observed in both concentrated solution and solid, which was ascribed to the dihedral angle change of binaphthyl moieties from solution to solid [39].

S-**2** was doped with polymethyl methacrylate (PMMA) to further investigate its photophysical behaviour in solid. As shown in Fig. 3a, with the increase of the molecule mass ratio, the emission peak had a significant redshift from 410 nm to 490 nm. When the mass ratio was 1:100, the emission at 410 nm was attributed to monomer. The spectra show that when the mass ratio was up to 3:100, the excimer emerged, and the emission peaks composed of both the excimer and monomer. While the mass ratio up to 6:100, the spectra showed that the emission peak at 410 nm from the monomer disappeared while the only emission from the excimer existed. To get further insight into the molecule, the optical properties in different ratios of H_2O and THF were examined. As evident from Fig. 3b, the main emission peaks at 410 nm were enhanced by the increase in water composition. Whereas the peaks at 410 nm sharply decreased and became negligible when the volume ratio of H_2O and THF reached 7:3 along with a peak at 510 nm showed up, which was corresponding with the fluorescence in solid. Similarly, the increase in water composition enhanced the intensity of peaks at 510 nm. Changes in the ratio of H_2O and THF resulted in a redshift (~100 nm) from 410 nm to 510 nm in spectra and the quantum yield Φ_F from 6.9%–27.6%, indicating the formation of excimer. The CD spectra in different volume ratios of H_2O and THF were conducted. In Fig. S9 (Supporting information), there was no obvious changes before the volume ratio reached 7:3. While the volume ratio up to 7:3, CD signal sharply fell, which was associated with the emission change. The possible reason was that the solution turbidity caused by the solubility decrease. A distinct colour change could be observed from blue to yellow-green under the UV light irradiation. The CPL spectra (Fig. 3c) revealed that the optical properties changed from single molecule to excimer. There was no CPL signal observed in

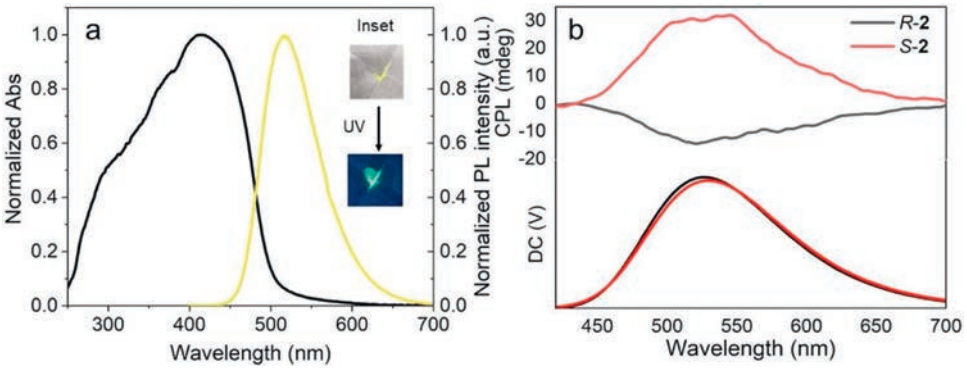

Fig. 1. (a) Normalized absorption spectrum of *R*/*S*-**2** in solid (black line). Normalized fluorescence spectrum of *R*/*S*-**2** in solid (yellow line, λ_{ex} = 350 nm). Inset: pictures of *R*/*S*-**2** under irradiation of daylight and UV. (b) CPL spectra of *R*/*S*-**2** in neat film (λ_{ex} = 350 nm).

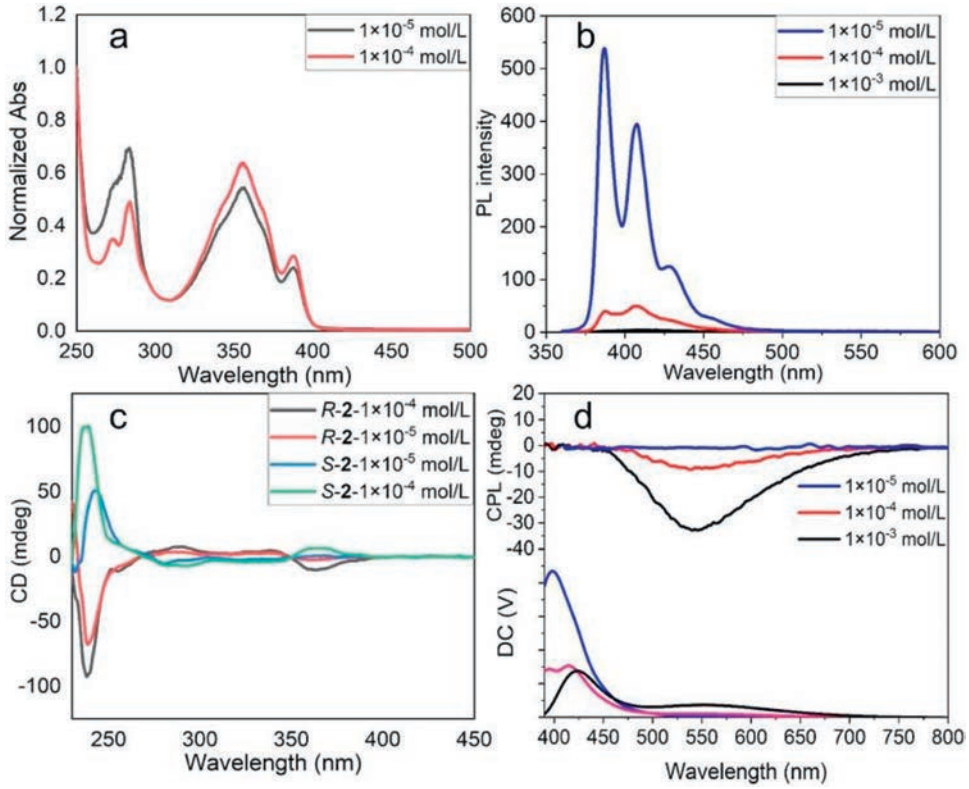

Fig. 2. (a) Normalized absorption spectra of *S*-**2** in THF. (b) Fluorescence spectra of *S*-**2** in THF at 1×10^{-5} mol/L (blue line), 1×10^{-4} mol/L (red line) and 1×10^{-3} mol/L (black line), λ_{ex} = 350 nm. (c) CD spectra of *R*/*S*-**2** at 1×10^{-5} mol/L and 1×10^{-4} mol/L. (d) CPL spectra of *S*-**2** at 1×10^{-5} mol/L, 1×10^{-4} mol/L and 1×10^{-3} mol/L in THF (λ_{ex} = 350 nm).

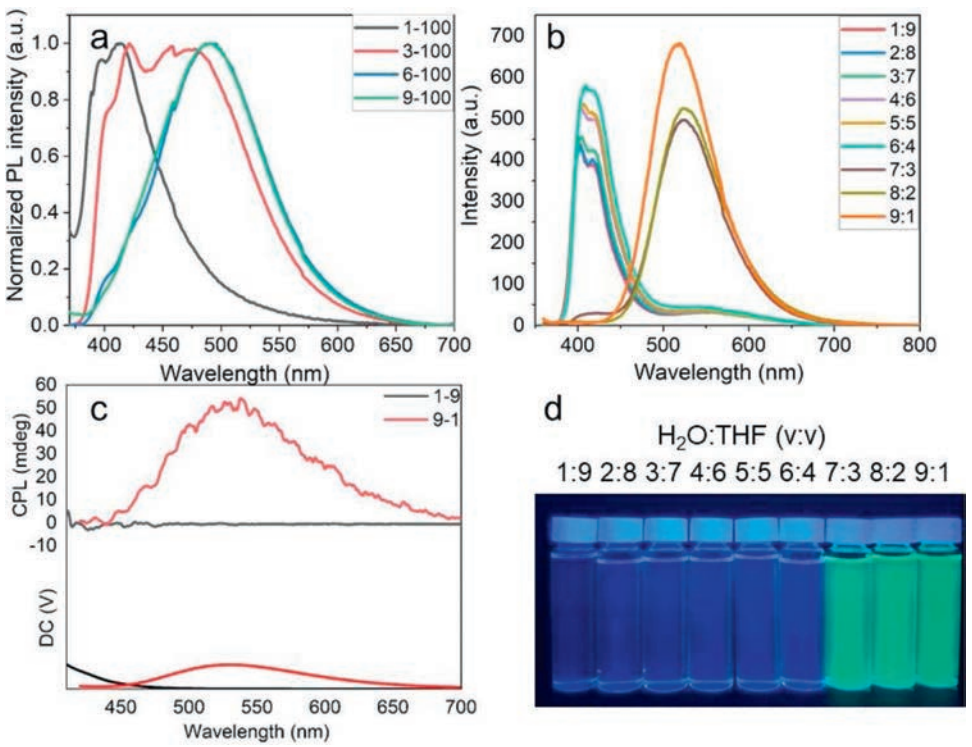

Fig. 3. (a) Fluorescence spectra of *S*-**2** doped with PMMA at the mass ratio of 1:100, 3:100, 6:100 and 9:100 (λ_{ex} = 350 nm). (b) PL spectra of *S*-**2** in different volume ratio of H_2O and THF (at a fixed concentration 1×10^{-5} mol/L, λ_{ex} = 350 nm). (c) CPL spectra of *S*-**2** in different volume ratio of H_2O and THF at 1×10^{-5} mol/L (λ_{ex} = 350 nm). (d) The pictures of *S*-**2** in different volume ratio of H_2O and THF at 1×10^{-5} mol/L under UV irradiation at 365 nm.

spectra while a prominent peak appeared when the water concentration approached 90% with a high dissymmetry factor ($|g_{lum}|$) value of 6×10^{-3}.

The SEM images shown in Fig. S10 (Supporting information) confirmed that no obvious self-assembly was observed. With increasing of H_2O, the SEM images have no obvious change even at the volume ratio of 7:3 where the emission changed. The image further verifies that the emission is not from the aggregates. The most stable structure of **2** was obtained *via* DFT calculations by b3lyp/6-311+G* level of theory (Fig. S11 in Supporting Information). The dihedral angle between the naphthalene rings was 100°, which was close to a typical binaphthyl structure. The pyrene units linked to binaphthyl were almost perpendicular to another, indicating the excimer originated from intermolecular interaction rather than the intramolecular one. Meanwhile, the LUMO (lowest unoccupied molecular orbital) and HOMO (highest occupied molecular orbital) orbital distribution demonstrated that the emission was originated from pyrene units.

In summary, we constructed bromobinaphthol-pyrene materials with high quantum $\Phi_{F,\ solid}$ up to 55.9% and g_{lum} value up to 4.3×10^{-3} in solid state. In this system, the emission derived from molecules in diluted solution hardly showed CPL signal. While the emission from excimer in solid or mixture solvent exhibited both strong CPL signal and high quantum yield Φ_F. Moreover, reversal CPL signal can be detected in both concentrated solution and solid due to the dihedral angle change of binaphthyl moieties. Meanwhile, the readily synthesised material showed AIE property. The multifunctional chiral materials with both high luminescence dissymmetry factor g_{lum} and high quantum yield Φ_F would be greatly contribute to the further application of CPL materials.

Declaration of competing interest

The authors declare no competing financial interest.

Acknowledgments

This work was financially supported by the National Natural Science Foundation of China (NSFC, Nos. 21788102, 21722603 and 21871083), Shanghai Municipal Science and Technology Major Project (No. 2018SHZDZX03), 'Shu Guang' Project supported by Shanghai Municipal Education Commission and Shanghai Education Development Foundation (No. 19SG26), the Innovation Program of Shanghai Municipal Education Commission (No. 2017-01-07-00-02-E00010) and the Fundamental Research Funds for the Central Universities. Prof. Y. Cheng from Nanjing University and Prof. P. Duan from National Center for Nanoscience and Technology are also acknowledged for their guidance and assistance.

References

[1] J.Y. Zhu, C.X. Li, P.Z. Chen, et al., Mater. Chem. Front. 4 (2020) 176–181.
[2] H. Chen, X. Yao, X. Ma, H. Tian, Adv. Opt. Mater. 4 (2016) 1397–1401.
[3] P.Z. Chen, Y.X. Weng, L.Y. Niu, et al., Angew. Chem. Int. Ed. 55 (2016) 2759–2763.
[4] N. Liu, P.Z. Chen, J.X. Wang, et al., Chin. Chem. Lett. 30 (2019) 1939–1941.
[5] D. Yan, D.G. Evans, Mater. Horiz. 1 (2014) 46–57.
[6] X. Yang, X. Lin, Y. Zhao, Y.S. Zhao, D. Yan, Angew. Chem. Int. Ed. 56 (2017) 7853–7857.
[7] Q. Xiong, C. Xu, N. Jiao, et al., Chin. Chem. Lett. 30 (2019) 1387–1389.
[8] R.D. Richardson, M.G.J. Baud, C.E. Weston, et al., Chem. Sci. 6 (2015) 3853–3862.
[9] Y. Zhang, X.Y. Wu, J. Han, Chin. Chem. Lett. 30 (2019) 1519–1522.
[10] J. Yuasa, T. Ohno, H. Tsumatori, et al., Chem. Commun. 49 (2013) 4604–4606.
[11] H.T. Feng, X. Gu, J.W.Y. Lam, Y.S. Zheng, B.Z. Tang, J. Mater. Chem. C. 6 (2018) 8934–8940.
[12] Z.G. Wu, H.B. Han, Z.P. Yan, et al., Adv. Mater. 31 (2019)1900524.
[13] Z. Ma, T. Winands, N. Liang, et al., Sci. China Chem. 63 (2019) 208–214.
[14] Z.P. Yan, X.F. Luo, W.Q. Liu, et al., Chem. Eur. J. 25 (2019) 5672–5676.
[15] X. Jin, Y. Jiang, P. Duan, M. Liu, D. Yang, Chem. Commun. 54 (2018) 4513–4516.
[16] X. Ma, J. Wang, H. Tian, Acc. Chem. Res. 52 (2019) 738–748.
[17] X. Qin, J. Han, D. Yang, et al., Chin. Chem. Lett. 30 (2019) 1923–1926.
[18] Y. Sang, J. Han, T. Zhao, P. Duan, M. Liu, Adv. Mater. 31 (2019) 1900110.
[19] B. Lu, S. Liu, D. Yan, Chin. Chem. Lett. 30 (2019) 1908–1922.
[20] Y. Lu, Y. Tang, H. Lin, et al., Chin. Chem. Lett. 29 (2018) 1541–1543.
[21] Y. Wang, X. Li, L. Yang, et al., Mater. Chem. Front. 2 (2018) 554–558.
[22] F. Song, Z. Xu, Q. Zhang, et al., Adv. Funct. Mater. 28 (2018) 1800051.
[23] X. Li, Q. Li, Y. Wang, et al., Chem. Eur. J. 24 (2018) 12607–12612.
[24] L. Ji, Q. He, D. Niu, et al., Chem. Commun. 55 (2019) 11747–11750.
[25] C. Xu, L. Xu, X. Ma, Chin. Chem. Lett. 29 (2018) 970–972.
[26] J. Han, D. Yang, X. Jin, et al., Angew. Chem. Int. Ed. 58 (2019) 7013–7019.
[27] Z. Jiang, X. Wang, J. Ma, Z. Liu, Sci. China Chem. 62 (2019) 355–362.
[28] J. Li, C. Yang, C. Huang, Y. Wan, W.Y. Lai, Tetrahedron Lett. 57 (2016) 1256 – 1260.
[29] K. Takaishi, M. Yasui, T. Ema, J. Am. Chem. Soc. 140 (2018) 5334–5338.
[30] Q.W. Zhang, D. Li, X. Li, et al., J. Am. Chem. Soc. 138 (2016) 13541–13550.
[31] C. Gao, S. Silvi, X. Ma, et al., Chem. Commun. 48 (2012) 7577–7579.
[32] K. Takaishi, K. Iwachido, R. Takehana, M. Uchiyama, T. Ema, J. Am. Chem. Soc. 141 (2019) 6185–6190.
[33] K. Takaishi, R. Takehana, T. Ema, Chem. Commun. 54 (2018) 1449–1452.
[34] Y. Ohishi, M. Inouye, Tetrahedron Lett. 60 (2019) 151232.
[35] S. Reiter, M.K. Roos, R. Vivie-Riedle, ChemPhotoChem 3 (2019) 881–888.
[36] Y. Wang, Y. Li, S. Liu, et al., Macromolecules 49 (2016) 5444–5451.
[37] S. Ito, K. Ikeda, S. Nakanishi, Y. Imai, M. Asami, Chem. Commun. 53 (2017) 6323–6326.
[38] D. Kaji, S. Ikeda, K. Takamura, et al., Chem. Lett. 48 (2019) 874–876.
[39] Y. Sheng, D. Shen, W. Zhang, et al., Chem. Eur. J. 21 (2015) 13196–13200.